Computational Materials Science 171 (2020) 109222

Contents lists available at ScienceDirect

Computational Materials Science

journal homepage: www.elsevier.com/locate/commatsci

Surface and electronic properties of rutile TiO_2 thin films coated with PbO_2

D.H.M. Azevedo[a], G.S.L. Fabris[b], J.R. Sambrano[b], J.M.M. Cordeiro[a,*]

[a] Department of Physics and Chemistry, School of Natural Sciences and Engineering, São Paulo State University, 15385-000 Ilha Solteira, SP, Brazil
[b] Modeling and Molecular Simulation Group – CDMF, São Paulo State University, 17033-360 Bauru, SP, Brazil

ARTICLE INFO

Keywords:
TiO_2
PbO_2
Semiconductors
Density functional theory
Binary films
Surface energy

ABSTRACT

Binary films of semiconductors have lots of potential applications in material science. Initially, these films were based on In_2O_3 but, because of its high coast, alternative materials to replace it have been intensely sought after. In this sense, TiO_2 and PbO_2 are both n-type degenerated semiconductors, which can be good alternatives due to its easy preparation and low cost. Its unique characteristics justify investigating the properties of films composed of both materials. Structural and electronic surface properties of thin films with crystallographic planes (0 0 1), (0 1 0), (1 0 1), and (1 1 0) of TiO_2 coated with PbO_2 (TiO_2/PbO_2), both in rutile form, have been investigated in this study. Pure TiO_2 and PbO_2 bulk and TiO_2 thin films have also been studied for comparison purposes. Periodic quantum mechanics DFT calculations have been performed using B3LYP hybrid density functional and taking into account long-range interactions. In both bulks, the energy near the top of the valence band comes mainly from the O 2p orbitals. In the PbO_2 the states in the lower energy region of the conducting band are basically composed of Pb 6s and 6p orbitals, while in TiO_2 those states come mainly from the Ti 3d orbitals. The relative stability of the TiO_2 thin films (surfaces) follows the sequence (1 1 0) > (0 1 0) > (1 0 1) > (0 0 1), but changes substantially in the TiO_2/PbO_2 binary thin films increasing as (0 1 0) > (1 0 1) > (0 0 1) > (1 1 0). Band gap energies of the four studied pure TiO_2 thin films are practically the same as the bulk. However, there is a remarkable decrease in the band gap energies of binary films compared to pure TiO_2 films. The decrease in the bottom of the conduction band is due to the contribution of Pb 6s and 6p orbitals at energies below the bottom of the conduction band of the pure TiO_2 films.

1. Introduction

Binary films of semiconductors have attracted a big deal of attention thanks to the possibility of achieving improved functional performances comparatively to those of the constituent components. Those films have too many applications in advanced technological fields such as optoelectronic, catalysis, sensing and solar cells [1–3]. Additionally, substantial changes in the electronic properties and surface activity are possible through doping and/or control of methods of synthesis [4].

Initially, that technology was based on In_2O_3 but its high price makes it prohibitive for many applications. Therefore, the search for alternative materials has been very intense for both theoretical and experimental researchers. In this sense, computational modeling and simulation are shown as important tools which can assist experimentalists in rationalizing and directing researches *in situ*. Both rutile TiO_2 and PbO_2 are an interesting class of materials in terms of electronic and optical properties and can be seen as a viable alternative for such applications. Its properties have been explored both for experimental technics and theoretical methods [5–12].

Rutile TiO_2 is a semiconductor with a wide band gap energy of about 3 eV which is used as a photocatalyst, in solar cells for production of hydrogen and electric energy, as a gas sensor, and in heterogeneous catalysis for catalytic conversion of a great variety of organic pollutants and gases, just for mention some of its applications [13,14]. It plays an important role in the biocompatibility of bone implants in addition to being efficient against microorganisms [14–16]. It has also applications related to the large value of its dielectric constant and the large dielectric anisotropy [17]. Its electronic structure is usually described in terms of an ionic model based on the ions Ti^{4+} and O^{2-}, although surface oxygen vacancies, which gives rise to two excess electrons, results on the reduction of Ti^{4+} to Ti^{3+} [7,18]. The TiO_2 valence band is mainly built of oxygen p states and the conduction band of empty titanium d states [6,19,20].

PbO_2 has emerged as an attractive material to be used as anode for direct oxidation of organic compounds thanks to its good stability under the high positive potentials required, temperature stability, and high oxygen evolution potential [5]. One of its main applications is as the active material of positive plates of the lead-acid batteries. Although, as

* Corresponding author.
E-mail address: joao.cordeiro@unesp.br (J.M.M. Cordeiro).

https://doi.org/10.1016/j.commatsci.2019.109222
Received 25 July 2019; Received in revised form 21 August 2019; Accepted 23 August 2019
Available online 28 August 2019
0927-0256/

everybody knows, Pb is a highly toxic, not environmentally friendly metal, nowadays there are efficient recycling techniques that prevent its disposal in the environment and makes its use safe. Add to that its low price and one have a material worth paying attention to. Rutile PbO_2 is a narrow band gap semiconductor [10,21,22]. These types of semiconductors are coloured or black when closed to stoichiometry, but may potentially become transparent when donor doped to high carrier concentrations, as it has been found for CdO [23,24], thanks to the blue-shift of the optical band gap, accordingly to the Moss-Burstein effect [25,26]. Besides this phenomenon, the dependence between the conduction band structure and the optical transparency has also been analysed [27,28]. In order to obtain optical transparency the transitions from the filled conduction band states to the next highest conduction band must lie above the threshold for visible light absorption. According to band structure calculations the rutile PbO_2 conductor behaviour arises from the superposition of the Pb 6s states in the conduction band and O 2p orbitals on the top of the valence band [11]. However, the concentration of n-type transporters changes too much according to the preparing conditions, fact that suggest the conductivity is caused by lack of symmetry as oxygen vacancies or substitution of surface oxygens by hydroxyl groups [11].

Coating a substrate with a layer of other material can affect the electronic structure and can thus change to some extent the surface properties of these systems [29–31]. In this work is being investigated the surfaces and electronic structures of TiO_2 films coated with PbO_2 via density functional theory (DFT) calculations, in the wake of a series of studies that have been developed in our laboratory since some time ago [32–38]. As far as we know, this is the first time this system is being investigated. Bulk of both neat PbO_2 and TiO_2 and surfaces of neat TiO_2 have also been simulated for comparison. The films have been computationally modelled in the crystallographic directions [1 1 0], [1 0 1], [0 1 0], and [0 0 1], and the analysis will be done in terms of optimized geometric parameters, band structure, density of states (DOS) structure analysis, distribution of charge density, and surfaces order stability of the coated films.

2. Model system

The crystalline rutile structure belongs to the tetragonal space group ($P4_2/mnm$), as shown in the Fig. 1, with 6 ions per primitive unit cell and cell parameters a and c, and internal u parameter. The internal u parameter is related to the vertical distance between an oxygen and a metal atom.

The experimental values of the TiO_2 parameters are $a = c = 4.594$ Å, $b = 2.959$ Å, and $u = 0.305$ Å [39], while they are $a = c = 4.958$ Å, $b = 3.338$ Å, and $u = 0.296$ Å, for PbO_2 [10]. The difference between the cell parameters of the two oxides is significative (about 0.3 Å), consequence of the difference between the metals atomic radius, which makes the convergence of the calculations for the coated TiO_2 thin films somewhat difficult. Even so, convergence is achieved for thick coatings of a few layers, which, from an experimental point of view, suggests an easy synthesis of the bi-layers films.

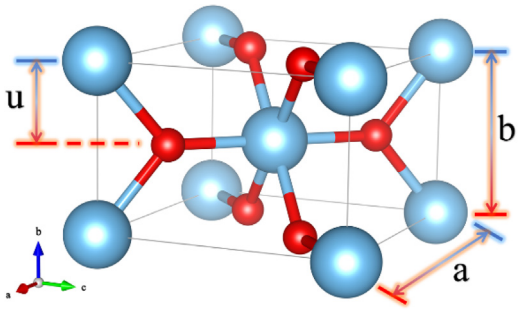

Fig. 1. The conventional rutile unit cell (blue: Pb or Ti; red: O).

To model experimental thin films, slabs with crystallographic planes with Miller indices ($h\,k\,l$) (0 0 1), (0 1 0), (1 0 1), and (1 1 0), were constructed from the bulk with the geometry previously optimized. The bulk was cut perpendicularly to the vector of the aimed direction, making a two-dimensional periodic structure with a finite number of layers in the c-direction. The slabs must be thick enough so that the interactions between the upper and lower faces are negligible. To find the minimum thickness required to satisfy this criterion, calculations are made with increasing thickness of the films up to achieve convergence in the surface energy [40]. Following that approach, simulations were performed with slabs having a thickness of approximately 25 Å, with little differences of thickness as a function of the crystallographic direction. It deserves to mention that, at variance with the procedure adopted in the plane waves codes, the system is truly a bi-dimensional crystal, that is, the slab model does not include images above and below the reference slab. The slabs are then submitted to geometry optimization in order to allow relaxation of the surface atoms and minimize de surface energy. Once the pure TiO_2 slabs have been simulated the Ti atoms on the two first layers of the surface are substituted for Pb atoms and the optimization procedure was repeated. For reasons of symmetry, which influences the convergence of calculations, the system effectively simulated was $PbO_2/TiO_2/PbO_2$; in other words, dividing the slab in half the two halves are a mirror image of each other. Values of the thickness of the slabs after relaxation are reported in Table 1. The number of layers is the same in all cases. A scheme of the simulated pure slabs and the surface Ti/Pb substituted ones is represented in Fig. 2.

3. Computational setup

The computational simulations were performed using the periodic DFT combined with hybrid functionals based on the generalized gradient approximation (GGA) [41,42]. Hybrid methods of density functionals have been widely used for molecules and also provide a good description of crystalline structures, such as bonding lengths and bonding energies, and band gap energy values in good agreement with experimental results. B3LYP [43,44] is one of the most popular hybrid functional used for studying solids. Several studies reveal that it describes a great set of molecules with good accuracy and high reproducibility [45–47].

The simulations were made with the CRYSTAL14 program [9], which uses Gaussian-type basis set to describe the crystalline orbitals [49]. Long-range interactions were also accounted through the Grimme approach [50,51] (namely B3LYP-D), which consider an increase in the total energy with a semi-empirical dispersion term [52]. More details can be found in a previous report [33]. A full optimization procedure (crystalline parameters $a = b$, and c, and inner coordinate u) was carried out for both bulk structures to determine the equilibrium geometry. Aiming to obtain better materials modelling, a couple of different basis set (chosen from the CRYSTAL basis set library http://www.crystal.unito.it/basis-sets.php) were tested both for Pb and Ti (see Table 2). Several basis set have also been tested for oxygen atoms. Unfortunately, it was not found a single basis set that could be used for both the oxides. Calculations with one of the oxygen basis set to both oxides lead to band gap and cell parameters that do not agree with the experimental ones for one of the oxides, leading to an inaccurate

Table 1
Thickness (Å) values for the different pure TiO_2 and TiO_2/PbO_2 thin films.

Planes	TiO_2	TiO_2/PbO_2
110	22.0	22.8
010	24.7	23.0
001	26.1	28.1
101	26.3	27.2

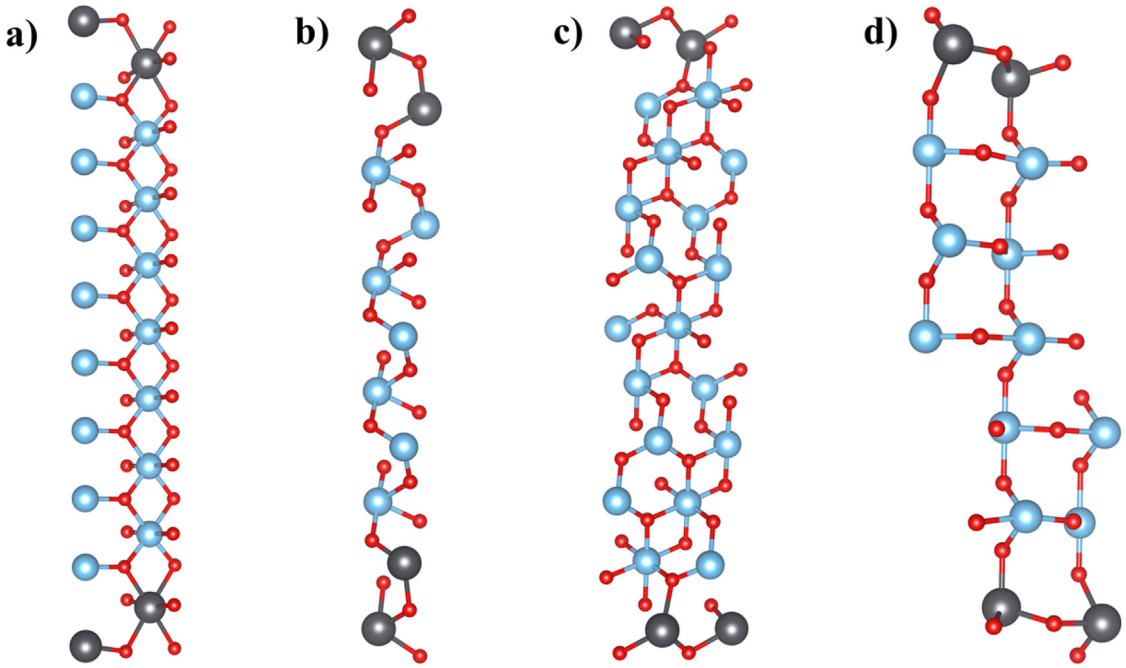

Fig. 2. Schemes of the (a) (0 0 1), (b) (0 1 0), (c) (1 1 0) and (d) (1 0 1) surface (blue: Ti; grey: Pb; red: O (in the case of pure TiO_2 films all metallic atoms are Ti).

description. Thus, two different basis set were used for oxygen, the 6-31d1 for PbO_2 [53], and the 8-411d1 for TiO_2 [54].

The bulk structure was optimized by the use of analytical energy gradients with respect to both atomic coordinates and unit cell parameters while the slabs were optimized with respect to the atomic coordinates only. The minimized structures were characterized by diagonalizing the Hessian matrix with respect to the lattice parameters and atomic coordinates; and the nuclear displacements and gradient components convergence were checked with tolerances on their root-mean-squares set to 10^{-3} and 10^{-4} a.u., respectively. The 10^{-10}, 10^{-10}, 10^{-10}, 10^{-10}, and 10^{-20} parameters were chosen for the Coulomb overlap, Coulomb penetration, exchange overlap, first exchange pseudo-overlap, and second exchange pseudo-overlap, respectively [33]. The shrinking (Monkhorst-Pack and Gilat) [55] factor was set up to 10. The percentage of Fock/Kohn-Sham matrices was kept at 80% and was also used the BROYDEN method to calculate only the first interactions [48], with a percentage of Fock/Kohn-Sham matrices changed to 50%.

4. Results and discussion

4.1. Bulk

Table 2 lists the calculated values of lattice parameters, inner coordinate, and band gap energy obtained with the different basis sets used for Ti and Pb, and the respective experimental values. Based on the results listed on the table, one can conclude that the 411(311d)G and DB-31G* (where DB refers to the Durand-Barthelat's pseudopotential) are the basis sets that fit better the experimental results shown for the bulks of TiO_2 and PbO_2 respectively, and were chosen to perform the remaining calculations. As a general found, it is noticed that the basis sets used for Ti overestimate the band gap energy values, while for Pb are found values larger and smaller than the experimental one.

Having chosen the most appropriated basis set to model the materials, it is possible to begin exploring theoretically its properties. The bulk band structure of both materials, to be used as a reference for posterior comparison (Fig. 3), has direct band gap at Γ point. It is easy to realize the huge difference in the behaviour and distribution of the bands from one material to the other. The PbO_2 upper valence band width is about 8.75 eV, in accordance with other theoretical values reported previously, 8.02 eV and 8.45 eV [10,11]. In turn, the TiO_2 upper valence band width is about 6 eV, which agrees well with early experimental data of 5.4 eV [62]. Thus, the valence orbitals in TiO_2 are distributed through a smaller energetic range than that of PbO_2, in strict agreement with the electronic distribution of the metal atoms. On the other hand, the conducting bands clearly reflect the difference in the conducting behaviour of the materials. That is a strong motivation to explore the influence of one material in the behaviour of the other, the aim of this study. In particular, PbO_2 presents a very characteristic conduction band, with a large gap of about 7 eV between the bottom of the band to the next lower portion of it on the Γ point, whose consequences on the optical behaviour of the material have been analysed previously [33].

According to what has been discussed by Walsh et al., the

Table 2
Experimental and calculated equilibrium lattice parameters and inner coordinate (Å) and band gap energy (eV) for neat rutile TiO_2 and PbO_2, using different basis sets for Ti and Pb.

TiO_2					PbO_2				
	a	*c*	*u*	E_g		*a*	*c*	*u*	E_g
Experimental [39]	4.594	2.959	0.305	3.06 [57]	Experimental [10]	4.958	3.338	0.296	0.61 [61]
411(311d)G [60]	**4.571**	**2.987**	**0.305**	**3.533**	**DB-31G*** [59]	**4.793**	**3.474**	**0.308**	**0.16**
86–411(31d)G [54]	4.627	2.982	0.306	3.705	211(1d)G [60]	4.801	3.256	0.308	1.485
86-51(3d)G [58]	4.591	2.966	0.305	3.789	6111(51d)G [56]	5.022	3.462	0.308	0.03

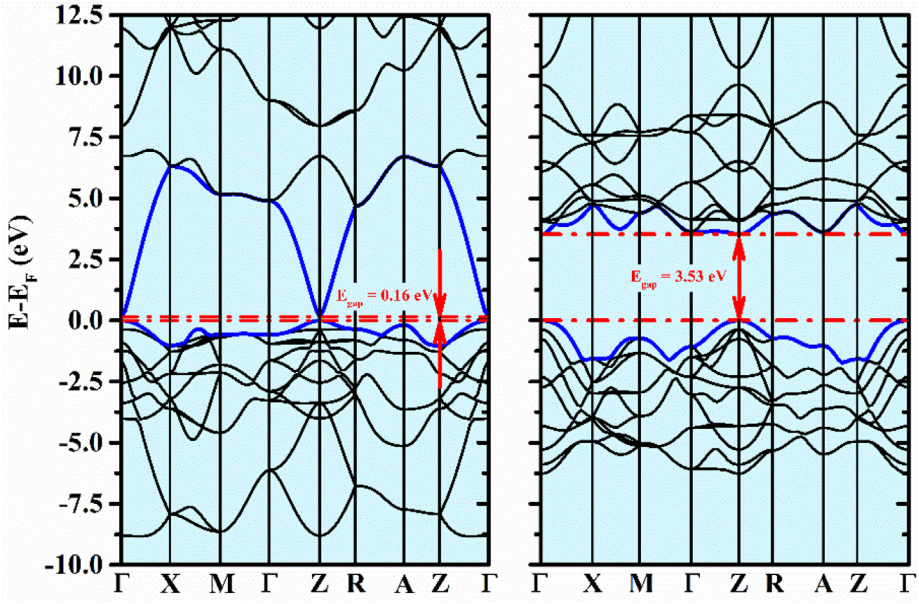

Fig. 3. Band structures of bulks of PbO_2 (left) and TiO_2 (right), with the energy scale set so that the Fermi level corresponds to 0.0 eV. The band structures were calculated along the high symmetry way of the Brillouin zone.

transparency of the PbO_2 could be manipulated, for instance, controlling the oxygen vacancies or doping, thanks to move the electron chemical potential inside the conduction band, and, consequently, changing the optical band gap energy [12].

Thus, the next natural step is to analyse the calculated density of states (DOS) profiles of each oxide to capture the contribution of the frontier atomic orbitals to the conducting behaviour of each of them. Those profiles are shown in the Fig. 4.

The agreement between these diagrams and experimental and theoretic ones published previously is outstanding. [9,11,19–21,62] In both TiO_2 and PbO_2 the O 2s orbital is responsible for the energy distribution in the lower range of the valence band (between −15 eV and −20 eV – not shown in the DOS diagram), corresponding to the lower energy levels in the band structure. In both cases, the energy near the top of the valence band comes mainly from the O 2p orbitals. As it is known, these orbitals are very localized, leading to small hole effective mass. This aspect, added to the small dispersion of the valence band, which makes it difficult the hole doping, is a strong reason for the n-type semi-conduction of these materials [63]. In the PbO_2 the states in the lower energy region of the conducting band are basically composed of spatially spread spherical Pb 6s, and 6p orbitals. Thus, electrons in PbO_2 have small effective masses and high electronic conduction is achieved. This is one reason why PbO_2 is a narrow band gap semiconductor [11,21,22]. Its charge transporters concentration is about 10^{21} cm^{-3} [10].

Unlikely, in TiO_2 those states come mainly from the Ti 3d orbitals. Because that the correct representation of the electronic properties of TiO_2 depends largely on the accurate representation of the O 2p and Ti

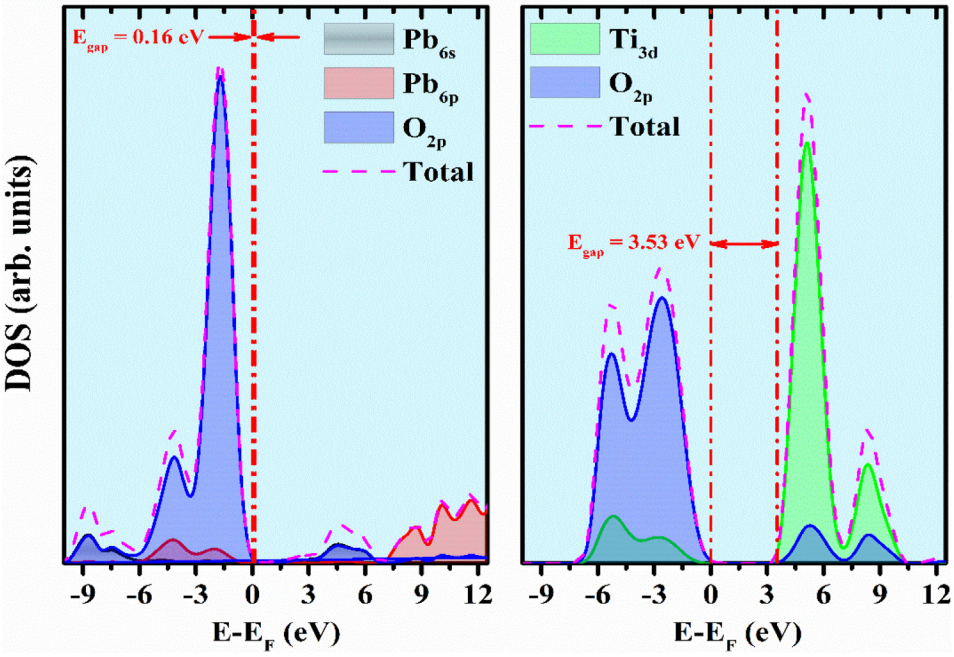

Fig. 4. Total and partial DOS diagram for PbO_2 (left) and TiO_2 (right).

3d orbitals. This is particularly important in the gap region where the range of interaction of O_{2p} and Ti_{3d} orbitals strongly influence the gap width [63]. As d orbitals have the energy level close to those of the O 2p orbitals they may form highly hybridized orbitals. That might raise the valence band maximum level and make hole doping easier, which might turn TiO_2 a p-type semiconductor [63]. The TiO_2 carrier concentration is about $10^{16}\,cm^{-3}$ [63]. Thus, it is noticed a remarkable agreement between the calculated results and the expected behaviour of both materials. On the other hand, the Ti 4s orbitals in TiO_2 do not contribute for the valence or conduction bands in the energy range investigated.

It deserves to pay attention that in both oxides the extreme metals s and d orbitals are empty (valence +4), that is, the metal ions are closed shell. It is clear than that the contribution of the atomic orbitals for the conduction band states and the electrical properties of the materials is strongly dependent on the atomic number of the metallic atoms. In PbO_2 is very explicit the separation of about 1 eV between the Pb 6s and Pb 6p conduction band states, with a region between about 7 and 8 eV where the density of states is virtually zero, as it has been reported previously, although in that case the range of zero density of states is between 4.2 and 5.8 eV [11].

Finally, in both cases is verified some penetration of orbitals of one band into the other, what agree with a hybridization of orbitals [11,63–65]. Thus, although in the electron distribution of the isolated metal atoms, the Ti d orbitals and Pb 6s and 6p orbitals are empty, as it has been said above, there is some distribution of charge through these orbitals in the oxides. That distribution will be directly related with the ionic/covalent character of the metal-oxygen chemical bond. Trying to rationalise the oxides behaviour related to the metal-oxygen bond it has been calculated the charge on the metal and oxygen atoms in each oxide, obtained through the Mulliken population analysis. The choice of Mulliken partitioning is arbitrary, since there is no unique method of performing the partition of the charge density. Paralleling, the results depend on the basis set used. Even so, the choice of a particular scheme is useful to support an analysis, especially when comparing different systems. The charges obtained for TiO_2 were 2.66 for Ti and −1.16 for O, while for the PbO_2 the charges on the atoms were 1.95 for Pb and −1.00 for O. These values lead to the conclusion that the Pb–O bonds in PbO_2 have a percentage of covalent character bigger than the Ti–O bonds, which are comparatively more ionic. That is because the larger size of the metallic atom in the PbO_2 results in a lower positive charge density, which leads to a lower charge transfer of the oxygen, whereas in the other case this electron transfer occurs in a greater extension. Consistently, while in the TiO_2 the O_{2p} – Ti_{3d} hybridization is verified in the energy range of 0 to −6 eV, in the PbO_2 the O_{2p} – Pb_{6s} and O_{2p} – Pb_{6p} hybridization covers a range of 10 eV. The O_{2p} – Pb_{6p} hybridization occurs in the upper energy range of the valence band (0 to −5 eV), while the O_{2p} – Pb_{6s} hybridization occurs in the lower energy range of the band.

4.2. TiO_2 surfaces

Hereafter, attention is focused on TiO_2 surfaces, since our purpose is to investigate the film properties of this material coated with PbO_2. It is well known that oxide films may exhibit properties significantly different from those of their bulks. In particular, there may be large changes in the band gap energy values of the material, including transitions from the indirect to direct type of the band gap, induced by 2D quantum confinement [66,67]. The study of surfaces permits to investigate the relationship between surface properties and the atomic surface distribution. The surface structure in metal oxide materials has a stronger influence on surface properties as compared to other metal or elemental semiconductors, because the mix of ionic and covalent bonding [14].

Fig. 5 shows the band structure calculated for these slabs. Although perhaps desirable, it is not shown the band structure in the same energy range shown for the bulk because the number of lines in the case of slabs is very large. Of course, this is a consequence of the great number of different neighbourhoods of each atom in the slabs.

That band structure is perfectly comparable with the first Γ – Γ interval (left side) of the bulk TiO_2 band structure (Fig. 3 – right) and differ little from those reported previously by Beltran and others using another basis set [68]. It is clear that the number of lines shown in both the valence and the conduction band is much larger in the slabs than in the bulk, in the corresponding energy range. Concomitantly, it is noticed also a minor change in the band gap value compared to that of the bulk. There is a slight increase of 0.1 eV in the case of the surfaces (0 1 0) and (1 0 1) and a slight decrease of 0.1 eV in the case of the surface (1 1 0). Interestingly, in the (0 1 0) and (1 0 1) surfaces the Ti atoms are 5-fold coordinated, while in the (1 1 0) surface the metal atom exhibits two coordination numbers: six and five.

These results suggest that there is a relation between the band gap of films and the coordination number of the surface metallic atoms, such that films whose surfaces have atoms less coordinated tend to have a band gap larger than the bulk, whereas films whose surfaces have atoms more coordinated tend to have a band gap smaller than that of the bulk. On the other hand, the surface (0 0 1) keeps the same value of the bulk band gap, however the band gap is tuned from direct to indirect (the direct band gap is 3.53 eV). In this case the surface Ti atoms are 4-fold coordinated. From the analysis of those results it is difficult to rationalise the relation between surface atom distribution or film crystalline direction and band gap variation. The changes in the band gap values are so small that any little change in the structure and/or in the electron distribution will cause those variations. It is valuable to have in mind that the bulk band gap energy can be seen as an average of the material band gap in the different crystallographic directions. Thus, it is not surprising that there are materials whose bulk band gap energy is very approximately equal to the band gap of the thin films grown in different crystallographic directions.

As a way of detailing the band structure let us starting to analyse the calculated density of states (DOS) profiles of each surface. These profiles are shown in the Fig. 6.

Just as in the bulk the main contribution to the valence band comes from oxygen 2p orbitals, whereas the conduction band is basically formed from Ti 3d orbitals. Also, as in the bulk, there is some contribution of 2p orbitals in the conduction band and 3d orbitals in the valence band, which denotes a certain degree of hybridization between these orbitals. Thus, from the point of view of the valence and conduction bands partition there is no significant change in the band structure between the bulk and the films. However, it is clear that the energy distribution of the orbitals, particularly the structure of the valence band, is strongly dependent on the growth direction of the films (minor differences are noticed in the conduction band, pointed to a homogeneous ambient of the charge transporters and a similar conductive behaviour for all of the slabs). As a general statement it can be said that the TiO_2 films conductive behaviour is quite similar to that of the bulk.

Of course, the growth direction of the films will dictate the surface energies in each case, since the surface distribution of atoms will be a function of the surface plane. Such energies will be a measure of the stability of the respective surfaces and will inform the preferred faces of growth of the crystals. The surface energy E_{surf} ($J.m^{-2}$) can be defined as the surface excess free energy per unit area and is a fundamental quantity to understand the direction of the crystal growth [52]. The standard method to calculate the E_{surf} is based on the equation $E_{surf} = (E_{slab} - nE_{bulk})/2A$, were E_{slab} and E_{bulk} are the total slab and bulk per oxide unit formula energies, respectively, n is the number of oxide units per unit cell, and A is the area of the unit cell [69]. The factor ½ arises from the existence of two faces on the film. This equation considers that the number of slab layers is large enough such that E_{surf} is not dependent of the slab thickness anymore.

The energies show the relative stability of the surfaces and then,

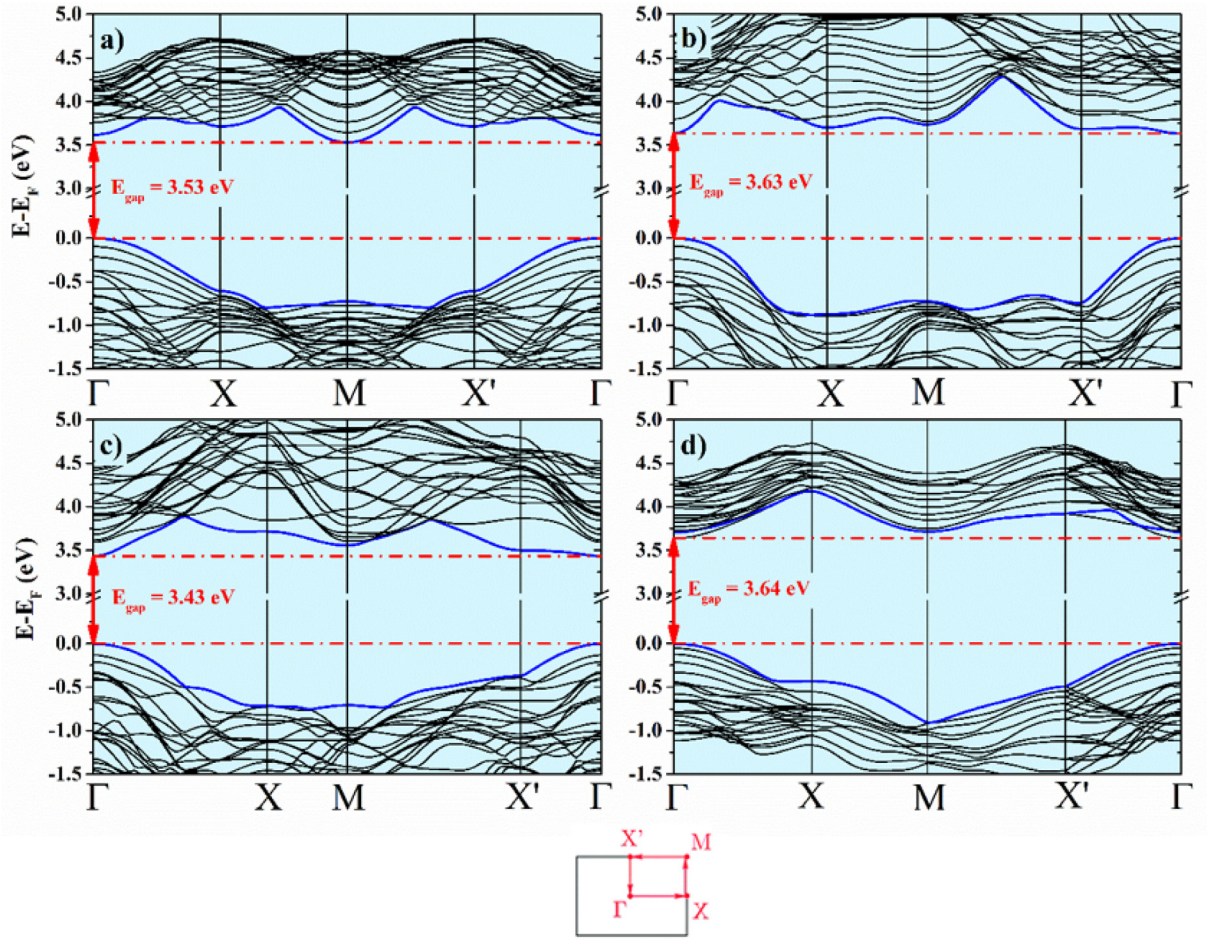

Fig. 5. Band structure of the TiO_2 surfaces: a) (0 0 1), b) (0 1 0), c) (1 1 0), and d) (1 0 1). The first Brillouin zone with high symmetry points for the surfaces is also shown below.

permit to estimate which is the face most favorable for the growth of the crystal grain. The values are listed in the Table 3 (the energies of the coated slabs will be object of analysis later). The surface stability obeys the sequence (1 1 0) > (0 1 0) > (1 0 1) > (0 0 1). Thus, the (1 1 0) crystal face is the most stable in the pure oxide, which agree with the thermodynamic behavior, and accounts for the highest content of the massive rutile TiO_2 surface. It is noticed a straight correlation between the surface energy and the coordination number of Ti in the surface. The Ti coordination number decrease from top to bottom from 6 to 4 (it is 5 for (1 0 1) and (0 1 0)), as it has been discussed above. Thus, the surface with Ti 6-fold coordinated is the most stable ((1 1 0)) and the TiO_2 crystals must growing preferentially in that direction.

The order of stability of the surfaces calculated in this work agree perfectly with that obtained previously for Barbosa et al. [70], although in our case the energies are higher than those. Apart from we have used different basis set to account for the atomic electrons we have also considered Grimme approach to takes into account atomics long range interactions in the calculations. Comparing to the previous results, this contribution to the surface energy decreases relatively from 30% to 14% of the total energy going from up to down in the Table 3. Considering those results is realized that the contribution of the long-range interactions to the surface energy is proportional to the surface atomic packing.

Using the rutile TiO_2 lattice parameters and the surface energies calculated it is possible to calculate the Wulff's solid of the oxide. The Wulff construction is based in the work of Gerge Wullf, developed in the early 20th century [71], and has been successfully used in materials science to obtain the shapes of materials [72–74]. The Fig. 7 shows the calculated and the natural crystal of it (a complete analysis of the scheme shown in this figure will be done in the next section). The agreement between the natural crystal (solid at the beginning of the line) [75] and the Wulff's solid calculated (at right of the previous) is quite good, which gives a high degree of reliability to the calculated surface energies and to the simulation as a whole. It deserves to mention also that the stability of the surfaces correlates perfectly well with the amplitude of the peaks in the powder X-ray diffraction published of the material [76]. The diffraction pattern shows that the surface (2 1 1), not studied in the present work, has an amplitude very similar to the (1 0 1) [76].

Table 4 lists the charge on the Ti and O atoms in the surface of the TiO_2 slab (the charges of the coated slabs will be object of analysis later). Remembering, the charges on the atoms for the TiO_2 bulk are 2.66 for Ti and −1.16 for O. It is necessary to point out that in the film each simulated atom has its own charge and, therefore, the charges on the metal and oxygen surface atoms do not cancel each other. The electric neutrality is verified through the film as a whole. Also, from the data in the Table 4 it is noticed that while the charge on the surface Ti atom becomes more positive, the charge on the O atom do not becomes more negative, as it would be expected. That asymmetry in the charge distribution is compensated as one goes deeper into the film. Analysing those results, one can conclude that although the charges on the atoms change from one slab to the other, in the average, the charge on the surface atoms decrease compared to the bulk. Thus, in the surfaces, the Ti–O bonds have a slight increase in the covalent character compared to the bulk.

These founds shown clearly that the semiconductor behaviour of the

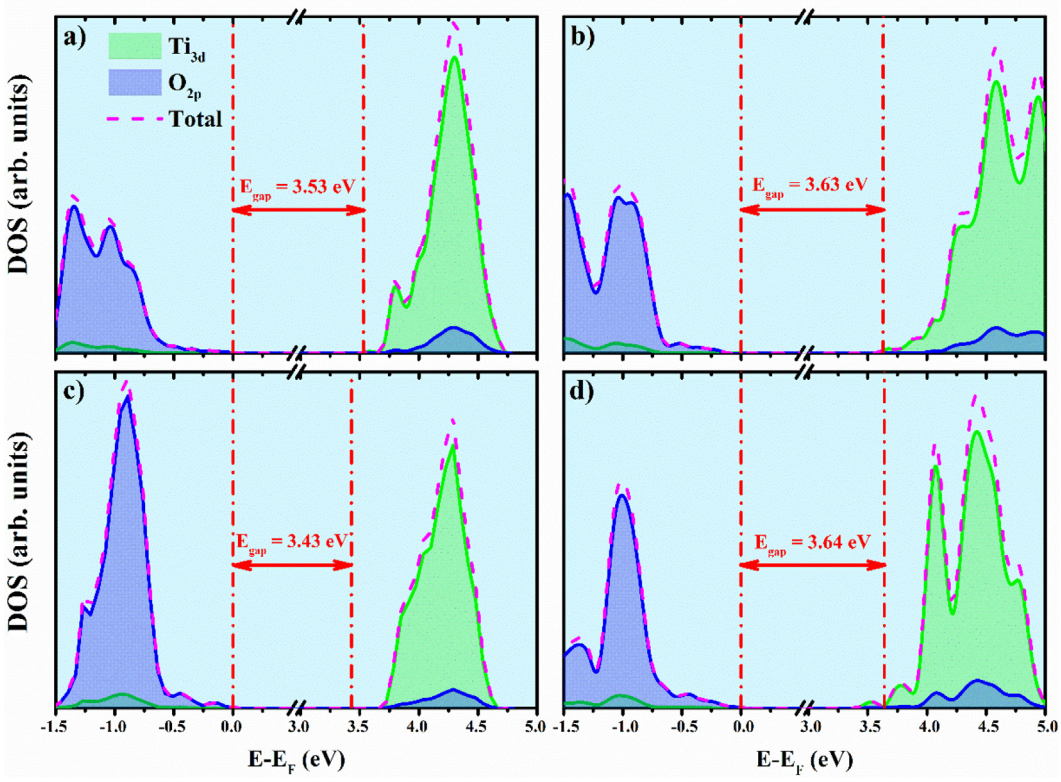

Fig. 6. Total and partial DOS diagram for neat TiO_2 surfaces: a) (0 0 1), b) (0 1 0), c) (1 1 0), and d) (1 0 1). Y axis is in arbitrary units.

Table 3
Surface energies (J/m^2) for TiO_2 and TiO_2/PbO_2 slabs.

Surface	TiO_2	TiO_2/PbO_2
(1 1 0)	0.96	1.59
(0 1 0)	1.21	0.49
(1 0 1)	1.47	0.82
(0 0 1)	1.85	0.96

Table 4
The atomic charge (e) on Ti and O atoms for pure TiO_2 and TiO_2/PbO_2 slabs.

Crystallographic planes	Pure		Coated	
	Ti	O	Ti	O
(0 0 1)	2.35	−1.13	2.66	−1.15
(0 1 0)	2.50	−1.04	2.69	−1.18
(1 0 1)	2.52	−1.05	2.68	−1.13
(1 1 0)	2.57	−0.99	2.72	−1.14

slabs, specifically the value of the band gap for each of them, is not affected by the charge distribution on the surface atoms. On the other hand, there is a perfect correlation between the charge on the atoms on each surface and the Ti coordination numbers, suggesting that these charges are mainly dictated by the surface atomic packing, in the sense that, as the coordination number of titanium on the surface increases, the charge on the atom increases. It is very interesting realizing that the positive charge on the Ti increase as the number of oxygen atoms around it increase, what seems to be very logical, since the oxygens have negative charge. On the other hand, these founds permit understand why the charge on the oxygen do not increase proportionally to the charge on the Ti, that is, the charge is distributed over a larger number of oxygen atoms and, so, each one has a smaller charge.

Thus, now the question is what changes will occur in the general behaviour of the films due to the surface coating with PbO_2.

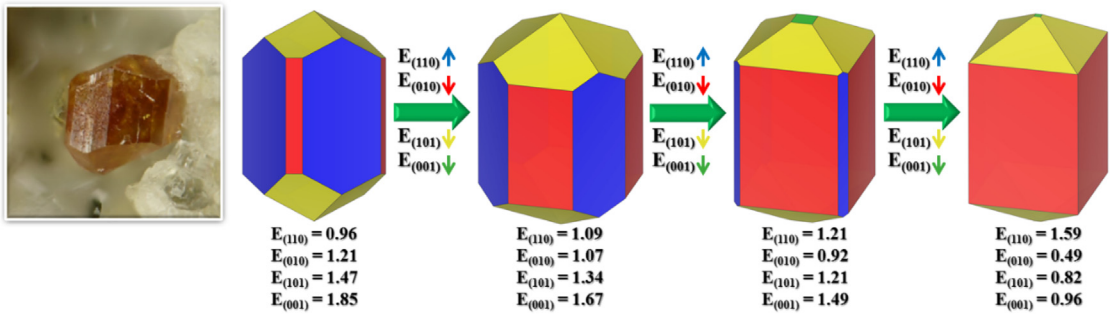

Fig. 7. Map of the morphology route leading from the pure TiO_2 to the TiO_2 coated with PbO_2. The pure oxide is changed to the coated one (surface energies shown in Table 3) through 2 randomly chosen steps of intermediate surface energies. The smaller arrows indicates a energy increase or decrease, and their color represents the respective surface. On the left is shown a photo of the mineral pure TiO_2 crystal [75].

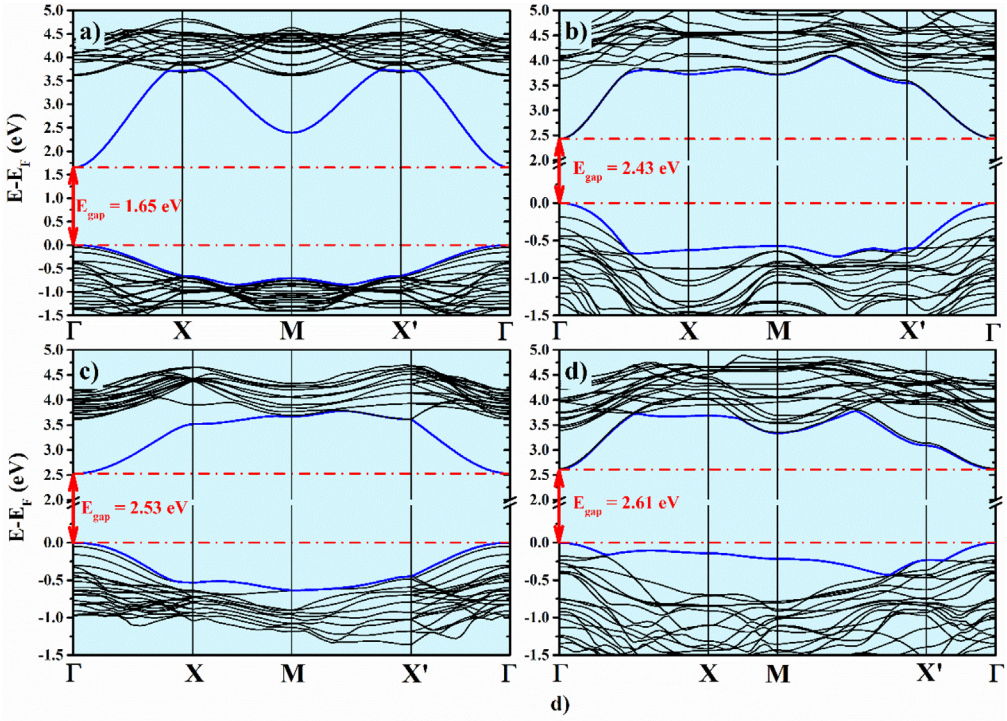

Fig. 8. Band structure of the TiO_2/PbO_2 slabs. Surfaces: a) (0 0 1), b) (0 1 0), c) (1 1 0), and d) (1 0 1). The first Brillouin zone with high symmetry points used to plot the structure band was the same used in the Fig. 5.

4.3. TiO_2 slabs coated with PbO_2

Let's start to analyze the changes in the properties of TiO_2 slabs due to the coating with PbO_2. The TiO_2/PbO_2 slabs have a thickness slightly larger than that of the pure TiO_2 ones (listed in Table 1), consequence of the larger radius of the Pb atom.

Fig. 8 shows the band structure calculated for the studied systems. Calculations were performed through the same Brillouin K-points used for the pure TiO_2 slabs. It is direct to notice the influence of the PbO_2 in the slab band gap, notably in the Γ point. The bottom of the conduction band structure is clearly dictated by the coating oxide. This imply in a significant decrease in the slabs band gaps comparing to the pure TiO_2 ones, which signify a better semiconductor behaviour of the TiO_2/PbO_2 slabs. It deserves to point out that while TiO_2 films, with a band gap of about 3.65 eV, absorb on the region of 340 nm of the electromagnetic spectrum (ultraviolet), the slabs will absorb from 475 nm (blue - surface (1 1 0)) up to 750 nm (red – surface (0 0 1)), depending on the film crystalline direction. Thus, incorporating of Pb on the TiO_2 slabs surfaces is an efficient method of modulating the films band gap. On the other hand, the energetic difference between the bottom level of the conducting band and the next one (about 2 eV for the (0 0 1) surface, 1.2 eV for surfaces (0 1 0) and (1 0 1), and 0.8 for surface (1 1 0)) suggests several possibilities to obtain different opto-electronic properties [10,12,33].

However, as the band gap energy is lower than 3.1 eV, it can be expected a lost in the films transparency comparing to the pure TiO_2, since electrons in the conduction band will be excited by visible light for the next conduction band, decreasing the optical transparency [27]. Table 5 lists the band gap variation between pure TiO_2 and TiO_2/PbO_2 slabs.

Table 5
The band gap variation (ΔE_g) for $E_g(TiO_2) - E_g(TiO_2/PbO_2)$ slabs.

Crystallographic planes	(0 0 1)	(0 1 0)	(1 0 1)	(1 1 0)
ΔE_g (eV)	1.88	1.20	1.03	0.90

It is noticed that the band gap variation changes to much from one slab to the other, however, there is no relation between the band gap variation and the direction of the film growth or the surface stability. This is a direct influence of the PbO_2 coating in the properties of the slabs. Looking for an atomic property that can be associated to the change in the band gap energy of the slabs it is listed the Ti and O atomic charges in the Table 4. As a first found is noticed that the film covering with Pb atoms leads to an increase in the atomic charges compared to the pure TiO_2 slabs. Thus, the Ti–O bonds in the matrix become more ionic with a consequent increase in the conductive character of the film. However, there is no direct relation between the atomic charges and the slabs band gap values, what confirms that the conductive character of the films is influenced mainly for the PbO_2 deposited on the surface. Interestingly, it is noticed a decrease in the Pb and oxygen charges (not shown), compared to the bulk oxide, denoting that the Pb–O bonds become more covalent than those of the pure material.

The DOS profiles of each slab permit to detail de atomic orbitals contribution for the valence and conduction bands of each slab. These profiles are shown in the Fig. 9. Similarly to the TiO_2 pure slabs, the valence band is constituted almost exclusively for oxygen 2p orbitals with Ti 3d orbitals contributing in a residual way, while the Ti 3 d orbitals are basically the only responsible for the conduction band. However, it is noticed a minor contribution of O 2p and Pb 6s orbitals (the contribution of the Pb 6p orbitals is even smaller) for the conduction band. As a way of detailing the contribution of the Pb orbitals to the variation in the slabs band gap relatively to the pure TiO_2 slabs, we have plotted only the contribution of those orbitals to the DOS structure. The plots for the slabs with the (0 0 1) and (0 1 0) surfaces, those which have the lower band gap, are shown in the Fig. 9 as insets. It is easy to realize the participation of Pb 6s and 6p orbitals to the decrease in the slabs band gap. They are responsible for the energy in a lower energy region of the conduction band unoccupied in pure TiO2, which reduces the band gap width.

Although in the Pb^{4+} the 6s and 6p orbitals are virtually empty,

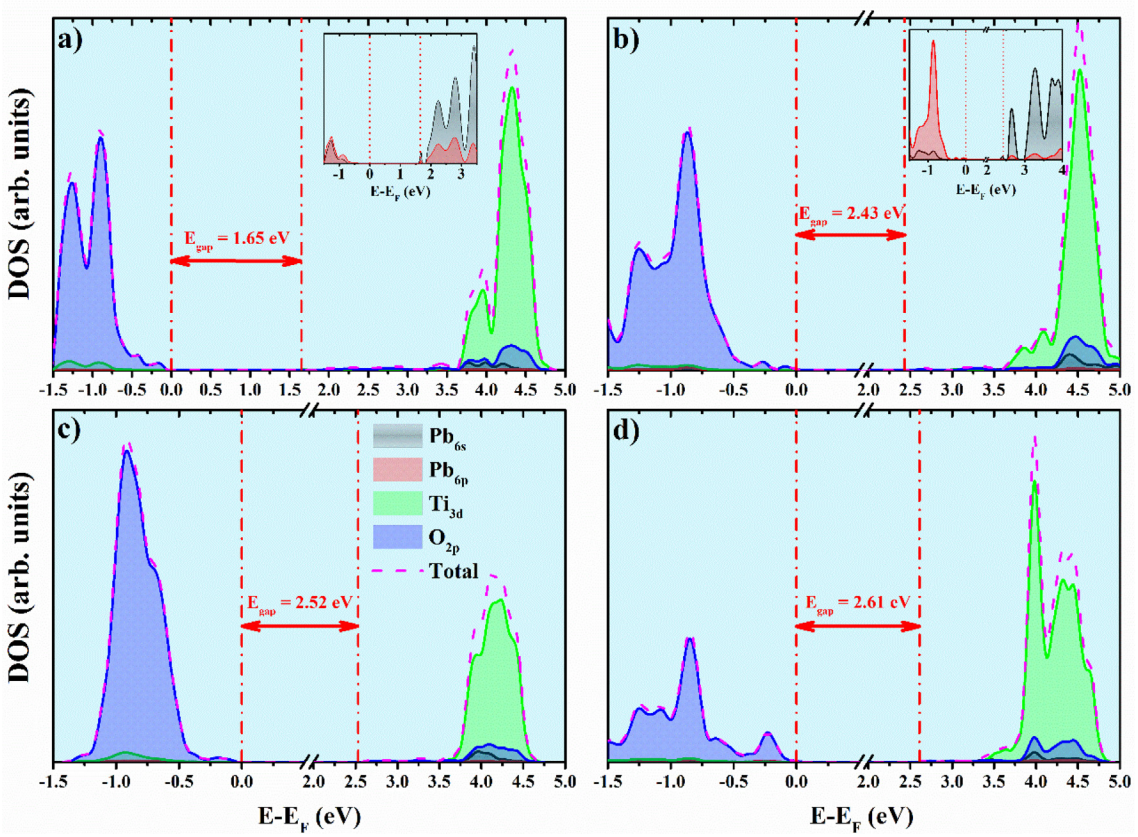

Fig. 9. Total and partial DOS diagram for neat TiO_2/PbO_2 surfaces: a) (0 0 1), b) (0 1 0), c) (1 1 0), and d) (1 0 1).

they are partially occupied in the films. According to the Mulliken charge calculations, about 2.1 electrons are distributed for those 2 orbitals. Comparing to the charge of the Ti atoms (Table 4), it is noticed that the Pb–O bond has a stronger covalent character than the Ti–O bond, which is more ionic. Being so it is the case now to have a look into the surface energy behaviour, and compare these energies with those of the pure TiO_2 slabs. With the coating it is noticed an atomic displacement leading to a new atomic distribution and consequent different surface energy compared to the pure slabs. In these cases, the surface energy is calculated according to the expression: $E_{surf} = (E_{slab} - n_1E_{TiO2} - n_2E_{PbO2})/2A$, where E_{slab} is the slab total energy, E_{TiO2} is the bulk energy of TiO_2 divided by the number of TiO_2 molecules in the bulk, n_1 is the number of TiO_2 molecules per slab, E_{PbO2} is the bulk energy of PbO_2 divided by the number of PbO_2 molecules in the bulk, n_2 is the number of PbO_2 molecules in the slab and A is the slab area.

In the Table 3 is listed the energies for each slab. The values show a radical change in the surface stability comparing to the neat TiO_2 slabs. As a general statement, whatever the surface it becomes more stable than that of pure slab. Curiously, preliminary calculations of the surface energy of pure PbO_2 slabs with the same crystalline directions, shown that the surfaces of PbO_2 are much less stable than those of TiO_2. Of course, changing Ti for a so huge atom like Pb, should provoke significant changes in the surface atomic distribution and it would be expected that this substitution would promote more or less perturbation as a function of the direction of growth of the film and the coordination number of the metallic atom on the surface. On the other hand, in the same preliminary calculations of the surface energy of pure PbO_2 slabs above mentioned, it is verified that the relative stability of the surfaces (although both oxides have the same crystalline structure) is not the same as for TiO_2 slabs. So, it is understandable that the relative stability of the surfaces changes comparing to the pure TiO_2 sequence. Changes in the sequence of TiO_2 surfaces stability have already been reported previously for the binary system TiO_2/SnO_2 [68]. As a consequence of this, a TiO_2/PbO_2 film will preferably grow in the direction favouring the surface (0 1 0). Taking into account the surface energies obtained it was calculated, using the Wulff's theory, the morphologic route leading from the pure TiO_2 to the TiO_2 coated with PbO_2, which scheme is shown in the Fig. 7.

It is known that morphologies can change as a function of surface stability. A given surface treatment can act in different ways in each of the surfaces, modifying the rate of growth in the respective directions [70]. The morphology transformations based on the modulation of the relationship between the surface stabilities of different faces and the areas of those parts which are exposed in the final shape has been explored previously by our group [70,72–74]. It is easy realizing that the morphology of the TiO_2 nanostructure is sensibly modified after coating with the PbO_2 film. Each face of the nanostructure is composed of a different termination and the characteristics of these faces govern the properties of the nanostructure. There is a vanishing of the surface (1 1 0), the surface (1 0 1) is maintained but changes to a pyramidal form and the surface (0 1 0) is more exposed, since it is the most stable. As it has already been commented, the band gap of the TiO_2 bulk can be understood as an average of the band gap of the respective film surfaces. In the same way, the approximate band gap of the new nanostructure might be a average band gap of the new crystalline faces. Considering the coated film band gap decreasing and the electronic properties of the faces, one can target new TCO applications, not favoured in the pure material.

5. Conclusions

Thin films of pure TiO_2 with faces (1 1 0), (0 1 0), (1 0 1), (0 0 1) and the films covered with PbO_2 have been simulated and the results compared to each other and with the bulk. The band gap energy of the pure films is practically the same of the bulk, but it changes

significatively in the covered ones. The top of the valence band of the pure films is composed of O 2p orbitals, while the bottom of the conduction band is composed of Ti 3d orbitals. High hybridization of these orbitals is noticed, which imply that there is some distribution of charge through 3d orbitals in the oxide. The surface stability obeys the sequence (1 1 0) < (0 1 0) < (1 0 1) < (0 0 1). It is noticed a straight correlation between the surface energy and the coordination number of Ti in the surface, in the sense that the higher the coordination number of Ti, the greater the surface stability. The Ti–O bonds of the films have a slight increase in the covalent character compared to the bulk. Concomitantly, there is a perfect correlation between the charge on the atoms on each surface and the Ti coordination numbers, suggesting that these charges are also dictated by the surface atomic packing.

Coating imply in a significant decrease in the films band gaps comparing to the pure TiO_2 ones. Thus, incorporating of Pb on the TiO_2 surfaces is an efficient method of modulating the films band gap. On the other hand, the energetic difference between the bottom level of the conducting band and the next one suggests several possibilities to obtain different opto-electronic properties. The Ti–O bonds in the matrix become more ionic with a consequent increase in the conductive character of the film. Pb–O bonds in PbO_2 are more covalent, while Ti–O bonds are comparatively more ionic. The analysis of the DOS shows that the Pb 6s and 6p orbitals are the responsible for decreasing the gap between the valence and conduction bands, because their energies are smaller than that of the Ti 3d orbital. As a general statement, whatever the surface it becomes more stable than that of pure slab and the order of surface stability changes for (0 1 0) > (1 0 1) > (0 0 1) > (1 1 0). The morphology transformation suggests new TCO applications, not favoured in the pure material.

CRediT authorship contribution statement

D.H.M. Azevedo: Software, Methodology, Visualization, Formal analysis. **G.S.L. Fabris:** Software, Validation, Visualization, Formal analysis. **J.R. Sambrano:** Conceptualization, Funding acquisition, Methodology, Project administration, Resources, Software, Writing - review & editing. **J.M.M. Cordeiro:** Conceptualization, Investigation, Methodology, Supervision, Project administration, Resources, Writing - original draft, Writing - review & editing.

Acknowledgments

This work is supported by Brazilian Funding Agencies: CNPq (46126-4), CAPES (787027/2013, 8881.068492/2014-01), FAPESP (2013/07296-2, 2016/07476-9). The computational facilities were supplied by Molecular Simulations Laboratory, São Paulo State University, Bauru, Brazil, and Laboratory of Computational Chemistry, São Paulo State University, Ilha Solteira, Brazil.

Data availability

The data needed to reproduce the findings are available in the body of the text.

References

[1] M.R. Hoffmann, S.T. Martin, W.Y. Choi, D.W. Bahnemann, Chem. Rev. 95 (1995) 69.
[2] A.L. Linsebigler, G.Q. Lu, J.T. Yates, Chem. Rev. 95 (1995) 735.
[3] T. Saito, T. Iwase, J. Horie, T. Morioka, J. Photochem. Photobiol. B 14 (1992) 369.
[4] X. Li, D. Pletcher, F.C. Walsh, Chem. Soc. Rev. 40 (2011) 3879.
[5] D.C. Moura, M. Cerro-Lopes, M.A. Quiroz, D.R. Silva, C.A. Martinez-Huitle, RSC Adv. 5 (2015) 31454.
[6] F. Labat, P. Baranek, C. Adamo, J. Chem. Theory Comput. 4 (2008) 341.
[7] P. Kruger, S. Bourgeois, B. Domenichini, H. Magnan, D. Chandesris, P. Le Fèvre, A.M. Flank, J. Jupille, L. Floreano, A. Cossaro, A. Verdini, A. Morgante, Phys. Rev. Lett. 100 (2008) 055501.
[8] P.D. Mitev, K. Hermansson, Surf. Sci. 601 (2007) 5359.
[9] D.J. Payne, R.G. Egdell, A. Walsh, G.W. Watson, J. Guo, P.-A. Glans, T. Learmonth, K.E. Smith, Phys. Rev. Lett. 96 (2006) 157403.
[10] D.O. Scanlon, A.B. Kehoe, G.W. Watson, M.O. Jones, W.I.F. David, D.J. Payne, R.G. Egdell, P.P. Edwards, A. Walsh, Phys. Rev. Lett. 107 (2011) 246402.
[11] D.J. Payne, R.G. Egdell, D.S.L. Law, P.-A. Glans, T. Learmonth, K.E. Smith, J. Guo, G.W. Watson, A.J. Walsh, Mat. Chem. 17 (2007) 267.
[12] A. Walsh, A.B. Kehoe, D.J. Temple, G.W. Watson, D.O. Scanlon, Chem. Commun. 49 (2013) 448.
[13] U. Diebold, Surf. Sci. Rep. 48 (2003) 53.
[14] V.M. Longo, F.C. Picon, C. Zamperini, A.R. Albuquerque, J.R. Sambrano, C.E. Vergani, A.L. Machado, J. Andrés, A.C. Hernandes, J.A. Varela, E. Longo, Chem. Rev. Lett. 577 (2013) 114.
[15] N.K. Awad, S.L. Edwards, Y.S. Morsi, Mater. Sci. Eng. C 76 (2017) 1401.
[16] K.S. Brammer, C.J. Frandsen, S. Jin, Trends Biotechnol. 30 (2012) 315.
[17] J. Pascual, J. Camasscl, H. Mathieu, Phys. Rev. B 18 (1978) 15.
[18] F. Guillemot, M.C. Port, C. Labrugere, C. Baquey, J. Colloids Interface Sci. 255 (2002) 75.
[19] D.O. Scanlon, C.W. Dunnill, J. Buckeridge, S.A. Shevlin, A.J. Logsdail, S.M. Woodley, C. Richard, A. Catlow, M.J. Powell, R.G. Palgrave, I.P. Parkin, G.W. Watson, T.W. Keal, P. Sherwood, A. Walsh, A.A. Sokol, Nature Mater. 12 (2013) 798.
[20] J. Szlachetko, K. Michalow-Maukeb, M. Nachtegaal, M.J. Sá, J. Chem. Sci. 126 (2014) 511.
[21] D.J. Payne, R.G. Egdell, G. Paolicelli, F. Offi, G. Panaccione, P. Lacovig, G. Monaco, G. Vanco, A. Walsh, G.W. Watson, J. Guo, G. Beamson, P.A. Glans, T. Learmonth, K.E. Smith, Phys. Rev. B. 75 (2007) 153102.
[22] D.J. Payne, R.G. Egdell, W. Hao, J.S. Foord, A. Walsh, G.W. Watson, Chem. Phys. Lett. 411 (2005) 181.
[23] M. Burbano, D.O. Scanlon, G.W. Watson, J. Am. Chem. Soc. 133 (2011) 1506515072.
[24] Y. Yang, S. Jin, J.E. Medvedeva, J.R. Ireland, A.W. Metz, J. Ni, et al., J. Am. Chem. Soc. 127 (2005) 8796.
[25] T.S. Moss, Proc. Phys. Soc. B 67 (1954) 775.
[26] E. Burstein, Phys. Rev. 93 (1954) 632.
[27] C. Kílíç, A. Zunger, Phys. Rev. Lett. 88 (2002) 095501.
[28] D. Segev, S.H. Wei, Phys. Rev. B 71 (2005) 125129.
[29] R. Inguanta, S. Piazza, C. Sunseri, J. Electrochem. Soc. 155 (2008) K205.
[30] P. Perret, T. Brousse, D. Belanger, D. Guay, J. Electrochem. Soc. 156 (2009) A645.
[31] P.N. Bartlett, T. Dunford, M.A.J. Ghanem, Mat. Chem. 12 (2002) 3130.
[32] J. Claverie, F. Bernard, J.M.M. Cordeiro, S. Kamali-Bernard, J. Phys. Chem. Solids 132 (2019) 48.
[33] J.M.M. Cordeiro, D.H.M. Azevedo, T.C.M. Barretto, J.R. Sambrano, Mat. Res. 21 (2018) e20170641.
[34] G.G. Almeida, J.M.M. Cordeiro, M.E. Martin, M.A. Aguilar, J. Chem. Theory Comp. 12 (2016) 1514.
[35] G.G. Almeida, A. Borges, J.M.M. Cordeiro, Chem. Phys. 434 (2014) 25.
[36] A. Borges, J.M.M. Cordeiro, Chem. Phys. Lett. 565 (2013) 40.
[37] J.M.M. Cordeiro, A.K. Soper, Chem. Phys. 381 (2011) 21.
[38] G.G. Almeida, J.M.M. Cordeiro, J. Braz. Chem. Soc. 22 (2011) 2178.
[39] R. Restori, D. Schwarzenbach, J.R. Schneider, Acta Crystallogr. B 43 (1987) 251.
[40] Albuquerque, A.R. Santos, I.M.G. Sambrano, J.R. Quim, Nova 37 (2014) 1318.
[41] J. Maul, A. Erba, I.M.G. Santos, J.R. Sambrano, R. Dovesi, J. Chem. Phys. 142 (2015) 014515.
[42] A.R. Albuquerque, A. Bruix, J.R. Sambrano, F. Illas, J. Phys. Chem. C. 119 (2015) 4805.
[43] A.D. Becke, J. Chem. Phys. 98 (1993) 56485652.
[44] C. Lee, W. Yang, G.R. Parr, Phys. Rev. B 37 (1988) 785.
[45] J. Tirado-Rives, W.L.J. Jorgensen, Chem. Theory Comp. 4 (2008) 297306.
[46] K. Lejaeghere, G. Bihlmayer, T. Björkman, P. Blaha, S. Blügel, V. Blum, et al., Science 351 (2016) 6280.
[47] S.F. Souza, P.A. Fernandes, M.J. Ramos, J. Phys. Chem. A 111 (2007) 10439.
[48] R.S. Dovesi, V.R. Saunders, C. Roetti, R. Orlando, C.M. Zicovich-Wilson, F. Pascale, B. Civalleri, K. Doll, N.M. Harrison, I.J. Bush, P.H. D'Arco, M. Lunell, CRYSTAL14 User's Manual Turin, University of Torino, 2014.
[49] C. Pisani, R. Dovesi, C. Roetti, Hartree-Fock Ab Initio Treatment of Crystalline Systems, Springer-Verlag, Berlin Heidelberg, 1988.
[50] S. Grimme, J. Comp. Chem. 25 (2004) 1463.
[51] S. Grimme, J. Comp. Chem. 27 (2006) 1787.
[52] A.R. Albuquerque, M.L. Garzim, I.M.G. Santos, V. Longo, E. Longo, J.R. Sambrano, J. Phys. Chem. A 116 (2012) 11731.
[53] C. Gatti, V.R. Saunders, C. Roetti, J. Chem. Phys. 101 (1994) 10686.
[54] F. Corà, Mol. Phys. 103 (2005) 2483.
[55] H.J. Monkhorst, J.D. Pack, Phys. Rev. B 13 (1976) 5188.
[56] G. Sophia, P. Baranek, C. Sarrazin, M. Rérat, R. Dovesi, Phase Trans. 86 (2013) 1069.
[57] J. Nowotny, Oxide Semiconductors for Solar Energy Conversion: Titanium Dioxide, CRC PRESS, Taylor and Francis, Boca Raton, FL, 2012.
[58] J. Scaranto, S. Giorgiann, J. Mol. Struct. Theochem. 858 (2008) 72.
[59] M. Nizam, Y. Bouteiller, B. Silvi, C. Pisani, M. Causa, R. Dovesi, J. Phys. C: Solid State Phys. 21 (1988) 5351.
[60] S. Piskunov, E. Heifets, R.I. Eglitis, G. Borstel, Comp. Mat. Sci. 29 (2004) 165.
[61] D.J. Payne, G. Paolicelli, F. Offi, G. Panaccione, P. Lacovig, G. Beamson, A. Fondacaro, G. Monaco, G. Vanko, R.G. Egdell, J. Electron Spectrosc. Relat. Phenom. 169 (2009) 26.
[62] A. Rubio-Ponce, A. Conde-Gallardo, D. Olguín, Phys. Rev. B 78 (2008) 035107.
[63] H. Hosono, Thin Solid Films 515 (2007) 6000.

[64] M.C.K. Sellers, E.G. Seebauer, Thin Solid Films 519 (2011) 2103.
[65] S.D. Mo, W.Y. Ching, Phys. Rev. B 51 (1995) 13023.
[66] A. Splendiani, L. Sun, Y. Zhang, T. Li, J. Kim, C.Y. Chim, G. Galli, F. Wang, Nano Lett. 10 (2010) 1271.
[67] K.F. Mak, C. Lee, J. Hone, J. Shan, T.F. Heinz, Phys. Rev. Lett. 105 (2010) 136805.
[68] A. Beltran, J. Andres, J.R. Sambrano, E. Longo, J. Phys. Chem. A 112 (2008) 8943.
[69] S.D. Lazaro, R.F. Penteado, S.M. Tebcherani, D. Berger, J.A. Varela, E.T. Kubaski, Quím, Nova 35 (2012) 920.
[70] M.A. Barbosa, G.S.L. Fabris, M.M. Ferrera, D.H.M. Azevedo, J.R.S. Sambrano, Mat. Res. 20 (2017) 920.
[71] G.Z.Z. Wulff, Kristallog 34 (1901) 449.
[72] A.F. Gouveia, M.M. Ferrer, J.R. Sambrano, J. Andrés, E. Longo, Chem. Phys. Lett. 660 (2016) 87.
[73] J. Andrés, L. Gracia, A.F. Gouveia, M.M. Ferrer, E. Longo, Nanotechnology 26 (2015) 405703.
[74] M.M. Ferrer, A.F. Gouveia, L. Gracia, E. Longo, Andrés, J. Model. Simul. Mat. Sci. Eng. 24 (2016) 025007.
[75] Hudson Institute of Mineralogy, available in: www.mindat.org/, access: 18/05/2016.
[76] K. Sakurai, M. Mizusawa, Anal. Chem. 82 (2010) 3519.